A Neuroprotective Peptide Modulates Retinal cAMP Response Element-Binding Protein (CREB), Synapsin I (SYN1), and Growth-Associated Protein 43 (GAP43) in Rats with Silicone Oil-Induced Ocular Hypertension.

Gretchen Johnson , Raghu Krishnamoorthy , Ram Nagaraj , Dorota Stankowska *

Posted Date: 11 October 2024

doi: 10.20944/preprints202410.0888.v1

Keywords: neuroprotection; peptain-1; αB-crystallin; CREB signaling; neurodegeneration; glaucoma; CPP-P1

Article

A Neuroprotective Peptide Modulates Retinal cAMP Response Element-Binding Protein (CREB), Synapsin I (SYN1), and Growth-Associated Protein 43 (GAP43) in Rats with Silicone Oil-Induced Ocular Hypertension

Gretchen A. Johnson [1,2], Raghu R. Krishnamoorthy [1,3], Ram H. Nagaraj [4] and Dorota L. Stankowska [1,2,*]

[1] North Texas Eye Research Institute, College of Biomedical and Translational Sciences, University of North Texas Health Science Center, Fort Worth, TX 76107
[2] Department of Microbiology, Immunology, and Genetics, College of Biomedical and Translational Sciences, University of North Texas Health Science Center, Fort Worth, TX 76107
[3] Department of Pharmacology and Neuroscience, College of Biomedical and Translational Sciences, University of North Texas Health Science Center, Fort Worth, TX 76107
[4] Department of Ophthalmology, School of Medicine, Anschutz Medical Campus, University of Colorado, Aurora, CO 80045
* Correspondence: dorota.stankowska@unthsc.edu; Tel.: 817-735-0239

Abstract: This study evaluated the neuroprotective potential of peptain-1 conjugated to a cell-penetrating peptide (CPP-P1) in an ocular hypertension model of glaucoma. Brown Norway (BN) rats were subjected to intraocular pressure (IOP) elevation via intracameral injection of silicone oil (SO), with concurrent intravitreal injections of either CPP-P1 or a vehicle. Retinal cross-sections were analyzed for markers of neuroprotection, including cAMP Response Element-Binding Protein (CREB), phosphorylated CREB (p-CREB), growth-associated protein-43 (GAP43), synapsin-1 (SYN1), and superoxide dismutase 2 (SOD2). Hematoxylin and eosin staining was used to assess retinal layer thickness. SO-treated rats exhibited significant reductions in the thickness of the inner nuclear layer (INL, 41%, p=0.016), inner plexiform layer (IPL, 52%, p=0.0002), and ganglion cell layer (GCL, 57%, p=0.001). CPP-P1 treatment mitigated these reductions, preserving INL thickness by 32% (p=0.059), IPL by 19% (p=0.119), and GCL by 31% (p=0.057). Increased levels of CREB and p-CREB were observed in IOP-elevated, CPP-P1-treated retinas compared to IOP-elevated vehicle-treated retinas. Although overall GAP43 levels were low, there was a modest increase in expression within the IPL and GCL in SO- and CPP-P1-treated retinas (p=0.15 and p=0.09, respectively) compared to SO- and vehicle-treated retinas. SO injection reduced SYN1 expression in both IPL and GCL (p=0.01), whereas CPP-P1 treatment significantly increased SYN1 levels in the IPL (p=0.03) and GCL (p=0.002). While SOD2 expression in the GCL was minimal across all groups, a trend toward increased expression was observed in CPP-P1-treated animals (p=0.16). The SO model was replicated with SO removal after 7 days and monitored for 21 days followed by retinal flat-mount preparation to assess retinal ganglion cell (RGC) survival. A 42% loss in RGCs (p=0.009) was observed in SO-injected eyes, which was reduced by approximately 37% (p=0.03) with CPP-P1 treatment. These findings suggest that CPP-P1 is a promising neuroprotective agent that promotes retinal ganglion cell survival and the preservation of other retinal neurons, potentially through enhanced CREB signaling in a rat model of SO-induced ocular hypertension.

Keywords: neuroprotection; peptain-1; αB-crystallin; CREB signaling; neurodegeneration; glaucoma; CPP-P1

 doi:10.20944/preprints202410.0888.v1

1. Introduction

It is estimated that nearly 112 million people worldwide will be living with glaucoma in the next 15 years [1]. Vision loss from glaucoma is currently irreversible due to progressive neurodegenerative effects that occur and the limited treatment options to prevent neurodegeneration. Damage comes from multiple facets, including an increased IOP that exerts various types of cellular and metabolic stress on the retina and pinches retinal ganglion cell (RGC) axons at the optic nerve head, leading to a progressive loss of RGCs starting in the periphery [2–4]. These output neurons are vital in transmitting visual information to the brain; thus, therapeutics that help preserve their function are greatly needed to sustain the quality of life of glaucoma patients.

A promising potential treatment has been designed from a well-studied family of chaperone proteins called α-crystallins known to activate numerous cellular cascades in response to stress to preserve cell integrity. These stress response proteins, also called heat shock proteins, are found in high concentrations in the eye lens [5–12]. Peptides derived from these proteins have also been assessed for pro-survival effects in various cell types. Alpha B-crystallin is a small heat shock protein studied for its chaperoning and anti-apoptotic effects. Peptain-1 (P1), a peptide derived from αB-crystallin, has been tested across multiple glaucoma models and found to be a potent neuroprotectant [7–9,11,13–29]. We have recently demonstrated that cell-penetrating peptide (CPP) conjugated to P1 (CPP-P1) displays improved cellular uptake and enhances neuroprotective effects in several models of RGC injury [30].

Several pathways were found to be upregulated in a recent transcriptomic analysis of adult primary RGCs from ocular hypertensive rats treated with CPP-P1 [30]. One member in some of these pathways, cAMP Response Element-Binding protein (CREB), is a known pro-survival transcription factor often activated following growth factor signaling [31–35]. In a rat model of bilateral common carotid artery occlusion, CREB was found to be decreased in ischemic rat retinas in addition to dysregulation of neurotrophic and inflammatory systems [36]. AAV-2-mediated Calcium/Calmodulin-Dependent Protein Kinase II (CaMKII) expression was found to increase the phosphorylation of CREB in RGCs to protect them from excitotoxic injury and optic nerve crush (ONC) injury [37]. One study proposed that extracellular vesicles derived from Schwann-Cells with activated CREB signaling pathways regulate reactive gliosis in rat retinas following optic nerve crush [38]. These recent studies highlight the beneficial role of CREB signaling through its downstream effects in various animal models of glaucomatous injury.

One of the downstream effects of CREB signaling in the brain is the activation of synaptogenesis and neuroplasticity pathways [32], which were found to be upregulated in the transcriptomic analysis in our previous work [30]. Growth-associated protein 43 (GAP43) and synapsin-1 (SYN1) are commonly used as markers of synaptogenesis and neuroplasticity [39,40]. Additionally, GAP43 is used as a biochemical marker of optic nerve regeneration in zebrafish and rodents [41–43]. SYN1 has been used as a marker of synaptic vesicle clustering [44], and its decreased activity has been noted in neurodevelopmental disorders [45]. While the precise effect of overexpression of synaptogenic genes in the retina is not fully understood, there could be a therapeutic window for maintaining RGC axon integrity. Investigating the expression of these two specific markers in the retina will help provide insight into the type of impact CREB activation may have on neuroprotection.

In addition to investigating CREB signaling, we examined the effects of CPP-P1 on mitochondrial function by evaluating the levels of the enzyme superoxide dismutase 2 (SOD2). By quenching superoxide, SOD2 acts as the mitochondrially relevant scavenger of reactive oxygen species, and an increase in its level was observed in the aqueous humor of POAG patients [46,47]. Increased expression of SOD2 was found by transcriptomics analyses in IOP-elevated Brown Norway rats [30], but the protein expression was not previously investigated within this experimental paradigm.

The current study aimed to validate previous RNA-seq findings in an SO model of acute intraocular pressure (IOP) elevation. Specifically, we wanted to confirm that the prospective neuroprotective drug, CPP-P1, increases CREB protein levels and CREB signaling as a mechanism underlying its beneficial effects.

 doi:10.20944/preprints202410.0888.v1

2. Materials and Methods

Animals

All animal procedures and protocols were carried out in accordance with the policies of the Association for Research in Vision and Ophthalmology (ARVO) resolution on the use of animals in ophthalmic and vision research and approved by the Institutional Animal Care and Use Committee (IACUC) at the University of North Texas Health Science Center. Brown Norway rats were purchased from Charles River and housed in the vivarium with controlled temperature, humidity, and constant dim light, with food and water provided ad libitum.

Peptide

CPP-P1 (VPTLK-DRFSVNLDVKHFSPEELKVK) was obtained from Peptide 2.0, Inc. (Chantilly, VA) at 95-98% purity. It was reconstituted in a vehicle (PBS), aliquoted, and stored in a 1 μg/μL stock concentration at -20°C.

Silicone Oil (SO) Model

The SO injection method described earlier [48–50] was used to induce ocular hypertension in one eye of Brown Norway rats, where the contralateral eyes were left untreated. Briefly, the rats (retired breeder 8-10 months, male) were anesthetized using the isoflurane induction @ 4% and maintenance @ 2.5% with 0.8-1 L oxygen level, and depth of anesthesia was ensured by the toe pinch reflex. One drop of 0.5% proparacaine hydrochloride was applied to the cornea as a topical anesthetic. An ultrafine 33-gauge needle was inserted through the cornea in the distal-temporal area about 2 mm from the limbus at a low angle to avoid contact with the iris. Once inserted, SO (Alcon Laboratories, Inc., Fort Worth, TX) was slowly released until a bubble filled the anterior chamber large enough to cover the pupil (about 20 μL). After the injection, the needle was held for one minute and gradually withdrawn from the anterior chamber. After the injection, a triple antibiotic ointment (bacitracin zinc, neomycin sulfate, and polymyxin B sulfate) was applied at the injection site, and the animals were allowed to recover from the anesthesia. Rats were housed with constant dim light (90 lux) throughout the duration of the experiment to reduce diurnal fluctuations in the aqueous outflow facility.

Intravitreal Injections of CPP-P1 or Vehicle

Following the SO injection, the IOP-elevated eye was subsequently injected with either CPP-P1 or vehicle using a Hamilton syringe. A single drop of 0.5% proparacaine hydrochloride (Alcon Laboratories, Inc., Fort Worth, TX) was applied to the injection eye. An ultrafine 33-gauge needle connected to a 10 microliter Hamilton syringe was used to intravitreally inject 2 μL of either CPP-P1 (2 μg) or vehicle into the vitreous chamber by insertion of the needle through the sclera, 1 mm behind the limbus region. The injection was carried out slowly, avoiding the lens during the needle insertion. After the injection, the needle was held for 1 minute and gradually withdrawn from the vitreal chamber. After the injection, a triple antibiotic (bacitracin zinc, neomycin sulfate, and polymyxin B sulfate) was applied at the injection site, and the animals were allowed to recover from the anesthesia. One week following the intravitreal injection in IOP-elevated eyes, animals were humanely euthanized by an overdose of 120 mg/kg body weight of Fatal-Plus (pentobarbital) (Covetrus, Dublin, OH) administered intraperitoneally followed by intracardial injection.

SO Removal Protocol and Tissue Collection Timeline

Briefly, the rats were anesthetized using the isoflurane induction @ 4% and maintenance @ 2.5% with 0.8-1 L oxygen level and ensured by toe pinch reflex. One drop of 0.5% proparacaine hydrochloride was applied to the cornea to reduce its sensitivity. Two ultrafine 33-gauge needles were used: one as a drainage needle and the other as an irrigation needle. The drainage needle was attached to a syringe without a pump to provide a route of oil outflow. The irrigation needle was attached to a syringe with irrigation solution (PBS) to flush the oil out. To do this, two incisions were made in the temporal quadrant of the cornea at the 2 and 5 o'clock positions at the edge of the oil

 doi:10.20944/preprints202410.0888.v1

droplet so that the tip of the drainage needle made contact with the oil. After slowly dispensing the irrigation solution and removing the oil, the drainage needle was first withdrawn, followed by the irrigation needle, and a small air bubble was injected into the anterior chamber to maintain a normal depth. The eye was pressed closed to close corneal incisions. After, a triple antibiotic (bacitracin zinc, neomycin sulfate, and polymyxin B sulfate) was applied at the injection site, and the animals were allowed to recover from the anesthesia.

IOP Measurements

IOP was measured 2-3 times a week with a TonoLab tonometer (Icare Finland Oy, Espoo, Finland) under isoflurane anesthesia. Each IOP measurement from the device was presented as the mean of six individual measurements, and ten IOP measurements were taken for each eye.

Pattern Electroretinography (PERG)

Pattern electroretinography (PERG) was performed following IOP elevation to assess the function of RGCs by measuring amplitude and latency, as described previously in our lab [51]. Rats were anesthetized (confirmed by toe pinch reflex) by isoflurane induction with SomnoFlo Electronic Vaporizer (Kent Scientific Corporation, Torrington, CT) @ 2.5% isoflurane and 600 mL/min oxygen and maintenance @ 2.5% isoflurane and 300 mL/min oxygen. The rats were subsequently placed on an adaptive heated stage. PERG measurements were conducted using the Jörvec instrument (Intelligent Hearing Systems, Miami, FL) and the Miami PERG system (Jörvec, Miami, FL) as previously described [30].

Immunohistochemistry of Retina Cross-Sections

The rat eyes used for histochemical analysis did not have the SO removed before euthanasia. Rat eyes were collected, fixed in 4% PFA, and then dehydrated in 70% ethanol overnight at 4°C, after which they underwent paraffin embedding in a TissueTek-VIP (Miles Scientific, Newark, DE). A Leica RM2255 Rotary Microtome (Leica Microsystems, Buffalo Grove, IL) was used to obtain 7-micron sections.

To stain the sections for the target proteins of interest, tissues were taken through deparaffinization by xylene for 5 min (two times), then a series of graded ethanol washes (100%, 95%, 80%, 70%, and 50%) for 5 min each. Next, antigen retrieval was performed by submersing slides in sodium citrate buffer and heating them to 72°C for 20 minutes. Subsequently, the slides underwent blocking for 60 min and were incubated in the primary antibody mixture at 4°C overnight in a humidified chamber. The following day, slides were washed in PBS three times for 10 min each and then incubated in the secondary antibody mixture (1:1000 dilution) at room temperature for 2 to 3 h in the dark. Slides were then incubated for 5 min in DAPI and rinsed thrice in PBS. They were then mounted with coverslips and sealed with nail polish to prevent drying. Slides were stained for CREB (CAT#9104S, Cell Signaling Technology, 1:250 dilution), p-CREB (CAT#9191S, Cell Signaling Technology, 1:250 dilution), GAP43 (CAT#335000, ThermoFisher, 1:250 dilution), SYN1 (CAT#515200, ThermoFisher, 1:250 dilution), and SOD2 (CAT#66474-1, ThermoFisher, 1:250 dilution).

Immunohistochemistry of Whole Retinal Flat-Mounts

The rat eyes described in this section had the SO removed before euthanasia. Eyes were enucleated and fixed in 4% PFA overnight at 4°C. Next, the retinas were carefully removed and cut at 4 positions to create quadrants for staining. Retinas were washed thrice in PBS and underwent a 5-minute permeabilization step before blocking for 60 min with blocking buffer (5% normal donkey serum and 5% BSA in PBS). Retinas were incubated in a primary antibody for 3 days at 4°C, washed thrice with PBS, and incubated in a secondary antibody for 1 h at room temperature. Retinas were then mounted with coverslips and sealed with nail polish to prevent drying. Slides were stored in the dark at 4°C after staining for RBPMS (GTX118619, GeneTex, 1:200 dilution). Images were taken using

 doi:10.20944/preprints202410.0888.v1

a fluorescent BZ-X series Keyence microscope (Keyence Corporation of America, Itasca, IL) and analyzed using ImageJ/Fiji (National Institutes of Health, Bethesda, MD).

Hematoxylin and Eosin Staining

The rat eyes used here did not have the SO removed before euthanasia. Slides were heated to 60°C for 1 h before being washed three times with xylene, each for 5 min. This was followed by washes in 100% ethanol twice for 2 min each, 95% ethanol for 2 min, and water once for 2 min. Next, they underwent hematoxylin (72511, ThermoFisher Scientific, Waltham, MA) staining for 3 min, a water wash for 2 min, a differentiator (mild acid) for 1 min, another water wash for 2 min, Bluing (Bluing Reagent, 7301, ThermoFisher Scientific, Waltham, MA) for 1 min, water wash for 2 min, 95% Ethanol for 1 min, and Eosin-Y stain for 30 sec. After Eosin-Y, slides were washed in 95% Ethanol for 5 min, then twice in 100% ethanol for 5 min each, and then two more washes in xylene for 15 min each.

Statistical Analysis

Statistical analyses were performed using GraphPad Prism 10 (GraphPad Software, La Jolla, CA). Unpaired t-tests were performed to assess differences between each group in IHC analysis; One-way ANOVA was performed for IOP data, cell counts, H&E data, and PERG data. Data were presented as mean ± standard error of the mean (SEM). P-values less than 0.05 were considered statistically different (*$p<0.05$, **$p<0.01$, ***$p<0.001$, ****$p<0.0001$).

3. Results

3.1. Intraocular Pressure (IOP)

Measuring IOP in the SO model is crucial for understanding the extent of ocular hypertension induced by the SO, which directly impacts the retinal changes observed; thus, we first assessed the IOP elevation to establish the severity of the induced condition before analyzing retinal outcomes. Our previous studies have shown that intravitreally administered CPP-P1 does not influence intraocular pressure [22,26]. In the current study, the average baseline IOP was 20.97 mmHg. Following SO injection, IOP increased significantly to an average of 30.47 mmHg ($p<0.01$). The data are presented as the change in IOP from baseline (Figure 1A).

3.2. Pattern Electroretinography (PERG)

To evaluate the impact of SO on retinal function, we measured pattern electroretinogram (PERG) responses in treated animals. The average baseline amplitude was 11.94 μV±0.57, with a latency of 60.13 ms±0.34, consistent with typical previously obtained values. Although measurements were attempted at the end of 7 days post-SO injection, they were inaccurate due to optical interference from the silicone oil (SO) in the anterior chamber of the rat eyes (Figure 1B,C). Therefore, SO was removed before performing PERG measurements in the second round of experiments.

3.3. CPP-P1 Prevented the Loss of Cells in the GCL

To assess the neuroprotective effects of CPP-P1 on RGCs in the first set of experiments, we quantified the cell density in the ganglion cell layer (GCL) by counting cells in retina cross-sections spanning from ora serrata to ora serrata and calculating the number per millimeter of the retina section across different treatment groups. The average number of cells in the ganglion cell layer (GCL) per millimeter was 56.8±2.13 in the naïve group, 27.5±1.60 in the SO + vehicle group ($p<0.0001$), and 43.7±2.00 in the SO + CPP-P1 group ($p=0.0002$) (Figure 1D). In the SO + vehicle group, IOP elevation induced by the SO model resulted in a significant 51% reduction in GCL cell density compared to the naïve group. However, treatment with CPP-P1 markedly mitigated this cell loss, reducing the decline by approximately 29%. These findings indicate that CPP-P1 provides substantial

 doi:10.20944/preprints202410.0888.v1

neuroprotection in the GCL, preserving a significant portion of retinal ganglion cells despite the elevated IOP induced by SO.

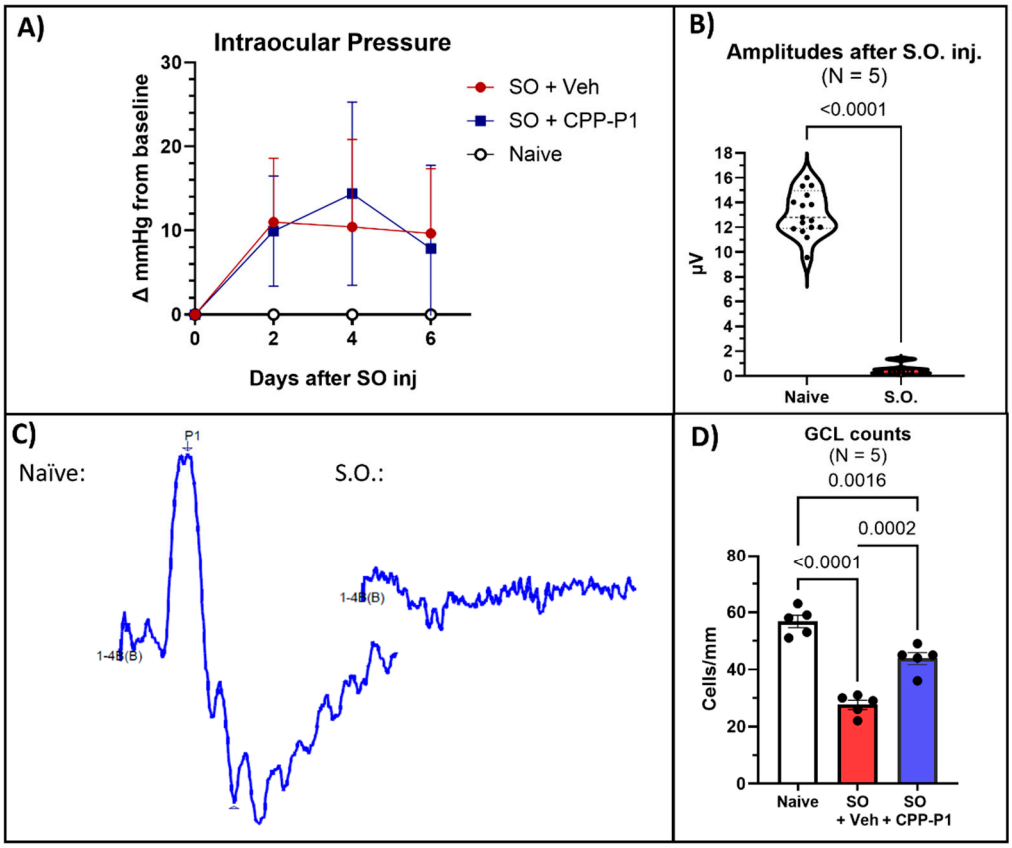

Figure 1. Damage produced by silicone oil (SO)-induced ocular hypertension and CPP-P1-mediated RGC protection. (**a**) Intraocular pressure (IOP) measurements indicated a significant ($p<0.01$) elevation of IOP occurred following SO injection. (**b**) Pattern Electroretinogram (PERG) amplitude measurements of healthy eyes (naïve) compared to those injected with SO. (**c**) Representative PERG graphs were obtained from the eyes with and without SO. (**d**) GCL counts from retinal cross-sections showed significant preservation of GCL cells with CPP-P1 treatment.

3.4. Retinal Layers Thickness

To evaluate the structural integrity of the retina, we measured the thickness of various retinal layers, including the outer nuclear layer (ONL), inner nuclear layer (INL), inner plexiform layer (IPL), ganglion cell layer (GCL), and overall retinal thickness. The retinal layers measured were reported in microns. In the naïve group, the average thicknesses were 36.4±2.21 μm for ONL, 24.1±1.77 μm for INL, 35.3±2.53 μm for IPL, 28.8±2.35 μm for GCL, and 127.5±8.70 μm for overall retinal thickness (Figure 2). In contrast, the vehicle-treated group displayed significant reductions, with averages of 32.5±2.02 μm for ONL, 14.3±1.60 μm for INL, 17.0±2.10 μm for IPL, 12.4±1.55 μm for GCL, and 82.4±8.34 μm for overall thickness, reflecting losses of 11% ($p=0.408$), 41% ($p=0.016$), 52% ($p=0.0002$), 57% ($p=0.001$), and 65% ($p=0.014$) respectively, compared to the naïve group (Figure 2A-E, Table 1).In the CPP-P1-treated group, the average thicknesses were 38.4±2.08 μm for ONL, 21.9±2.38 μm for INL, 23.8±2.07 μm for IPL, 21.3±3.12 μm for GCL, and 113.6±11.09 μm for overall retinal thickness. Compared to the naïve group, this corresponded to losses of 0% for ONL, 9% for INL, 26% for IPL, and 11% for overall thickness (Table 1). CPP-P1 treatment demonstrated appreciable preservation of retinal layer thickness when compared to the vehicle group, with the following reductions in layer thinning: ONL ($p=0.159$), INL ($p=0.059$), IPL ($p=0.119$), GCL ($p=0.057$), and overall retinal thickness ($p=0.090$). These results suggest that CPP-P1 offers significant protective effects against retinal thinning in this model.

 doi:10.20944/preprints202410.0888.v1

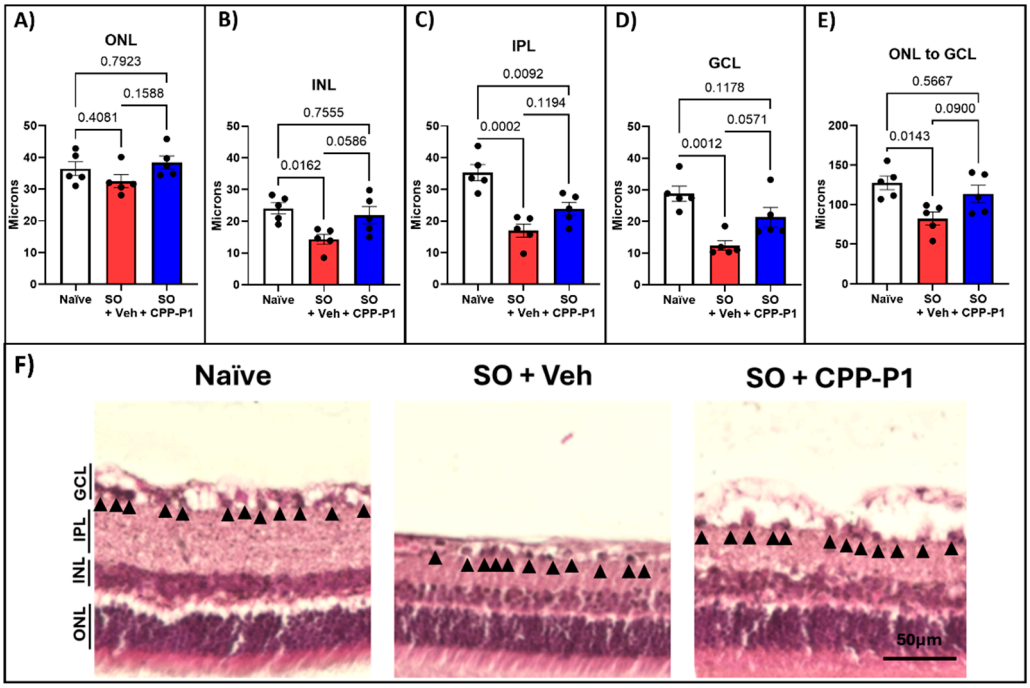

Figure 2. Retinal layer thickness measurements following H&E staining. Thickness measurements were taken from the (a) Outer Nuclear Layer (ONL), (b) Inner Nuclear Layer (INL), (c) Inner Plexiform Layer (IPL), (d) Ganglion Cell Layer (GCL), and (e) Total Retinal Thickness. (f) Representative images illustrate the significant loss of retinal thickness following SO injection and the preservation of retinal layers with CPP-P1 administration. Scale bar 50 µm.

Table 1. Quantification of retinal layer thickness following H&E staining. *p<0.05, **p<0.01, ***p<0.001.

Group	% loss in Vehicle	p-value Vehicle: Naïve	% loss in CPP-P1	p-value CPP-P1: Vehicle	p-value CPP-P1: Naïve
ONL	11%	0.408	0%	0.159	0.792
INL	41%	*0.016	9%	0.059	0.756
IPL	52%	***0.0002	33%	0.119	**0.009
GCL	57%	***0.001	26%	0.057	0.118
Total	65%	*0.014	11%	0.090	0.567

3.5. CREB and Phospho-CREB Analysis

Given the critical role of CREB in mediating neuroprotective and survival pathways within retinal neurons, we assessed its expression levels in the ganglion cell layer (GCL) across different treatment groups. CREB expression in the GCL was quantified by measuring the integrated density using ImageJ. Both the naïve and SO + vehicle groups exhibited similarly low levels of CREB expression (Figure 3A). However, in the SO + CPP-P1 group, CREB expression was higher than the naïve group, approaching statistical significance (p=0.09). Additionally, the naïve group displayed approximately twice the phosphorylated CREB (p-CREB) expression relative to CREB (Table 2). In contrast, the SO + vehicle group demonstrated a reduced p-CREB to CREB ratio, with p-CREB levels approximately half of those observed in the naïve group (p=0.17). Notably, the SO + CPP-P1 group maintained p-CREB expression similar to the naïve group (p=0.86) (Figure 3B). These findings suggest that CPP-P1 treatment may enhance CREB activation, potentially contributing to its neuroprotective effects in the GCL under conditions of SO-induced stress.

 doi:10.20944/preprints202410.0888.v1

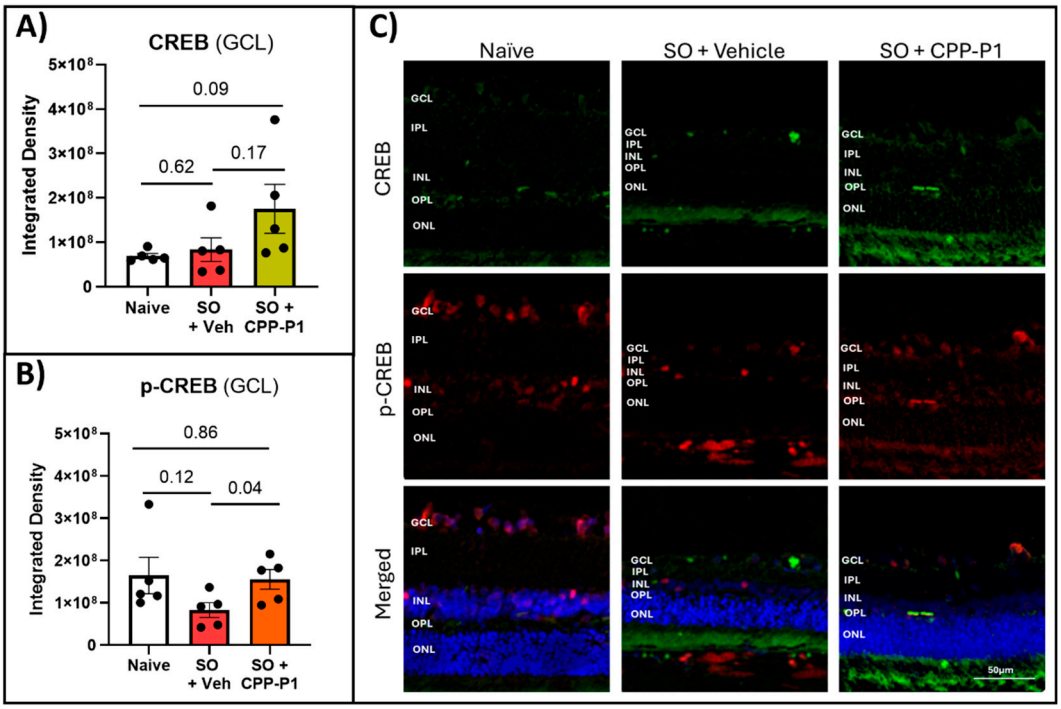

Figure 3. CREB and p-CREB levels in the experimental retinas. (**a**) CREB fluorescence in GCL, (**b**) p-CREB fluorescence in GCL. p-CREB levels were significantly elevated with CPP-P1 treatment compared to the vehicle-treated group. (**c**) Representative images, CREB (green), p-CREB (red), DAPI (blue). Scale bar 50 µm.

Table 2. Analysis of CREB expression levels in the experimental retinas. The table presents the relative CREB and phosphorylated CREB (p-CREB) levels in each experimental group, expressed in arbitrary units. Additionally, the ratio of p-CREB to total CREB is provided. Statistical significance is indicated by *p<0.05.

	Naïve	p-value Vehicle: Naïve	Vehicle	p-value CPP-P1: Vehicle	CPP-P1	p-value CPP-P1: Naive
CREB	6.9E7	0.62	8.3E7	0.17	1.8E8	0.09
p-CREB	1.6E8	0.12	8.3E7	*0.04	1.6E8	0.86
p-CREB/ CREB	2.3		1		0.9	

3.6. Expression of GAP43 and SYN1s following IOP Elevation and Treatment with CPP-P1

GAP43 is a critical marker of neuronal growth and synaptic plasticity, making its analysis essential for understanding the neuroprotective effects of CPP-P1 treatment in retinal neurons under stress conditions. GAP43 expression was quantified by measuring integrated density in the IPL and GCL. No significant differences were observed in GAP43 expression between the naïve and IOP-elevated, vehicle-treated groups. However, there were trends toward increased GAP43 expression in rats treated with CPP-P1 following IOP elevation, compared to vehicle-treated rats, in both the IPL and GCL (p=0.15 and p=0.09, respectively) (Figure 4).

 doi:10.20944/preprints202410.0888.v1

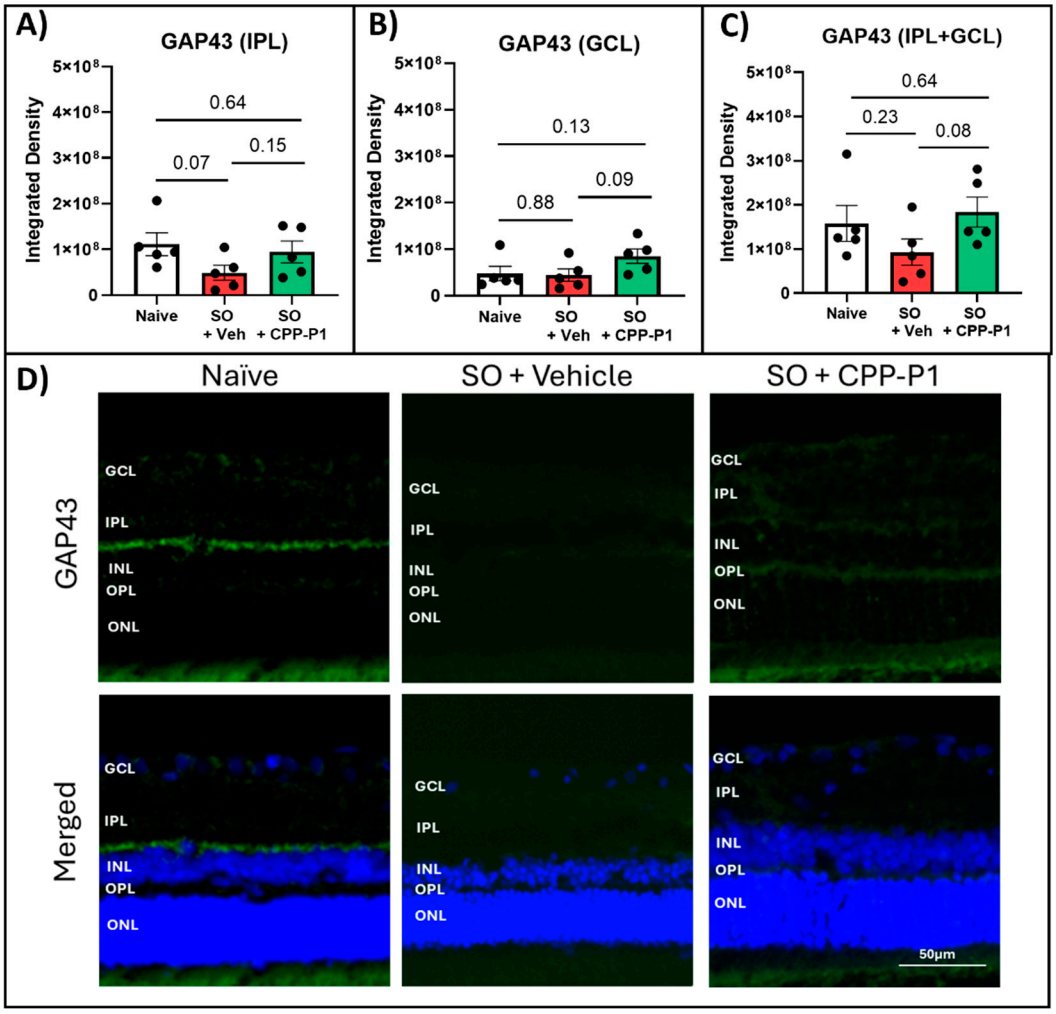

Figure 4. Expression of synaptogenesis marker GAP43. GAP43 expression levels are shown in the (**a**) Inner Plexiform Layer, (**b**) Ganglion Cell Layer, (**c**) Combined Inner Plexiform Layer and Ganglion Cell Layer with (**d**) Representative images, GAP43 (green), DAPI (blue). Scale bar 50 µm.

To gain a more comprehensive understanding of the neuroprotective effects of CPP-P1, we extended our analysis to include SYN1, a crucial protein in synaptogenesis and synaptic function, in addition to GAP43. SYN1 expression was measured by integrated density in the IPL and the GCL. There was a notable expression of SYN1 in the naïve IPL and a much lower expression in the GCL compared to GAP43. This expression significantly declined in the vehicle-treated group in the IPL ($p=0.01$), and a similar trend of decreased SYN1 expression was observed in the GCL ($p=0.21$). Rats treated with CPP-P1 showed significant increases in SYN1 in both IPL ($p=0.03$) and GCL ($p=0.002$) compared to the vehicle-treated group (Figure 5).

 doi:10.20944/preprints202410.0888.v1

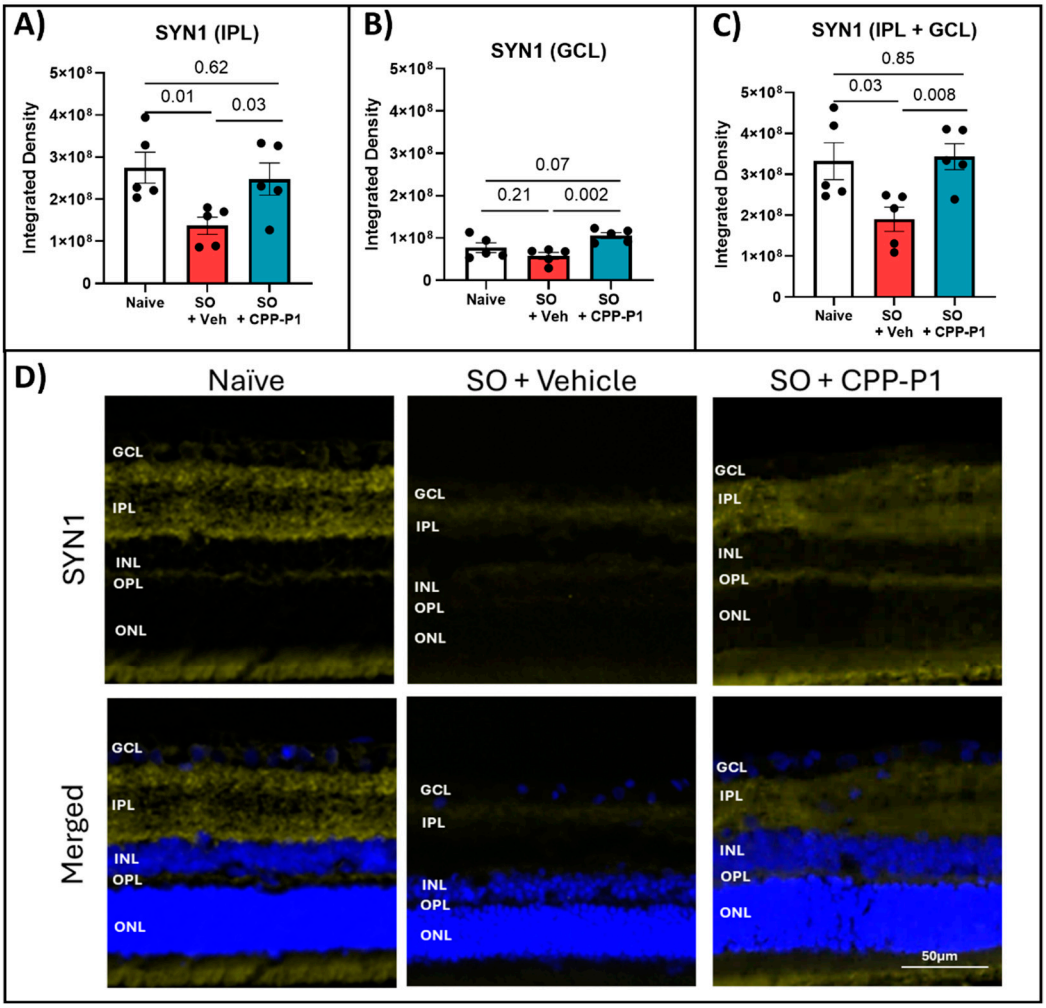

Figure 5. Expression of synaptogenesis marker SYN1 in the IPL and GCL. (**a**) Inner Plexiform Layer measurements, (**b**) Ganglion Cell Layer, (**c**) Combined Inner Plexiform Layer and Ganglion Cell Layer, (**d**) Representative images. SYN1 expression was significantly increased in both the IPL and GCL following CPP-P1 treatment. SYN1 (yellow), DAPI (blue). The scale bar 50 µm.

3.7. Mitochondrial SOD2 Levels Evaluation

SOD2 is a key mitochondrial enzyme that protects cells from oxidative stress by converting superoxide radicals into hydrogen peroxide and oxygen. In the retina, where high metabolic activity increases vulnerability to oxidative damage, assessing SOD2 expression helps reveal the mitochondrial response to stress and the potential antioxidant benefits of CPP-P1 in preserving retinal health under elevated intraocular pressure. SOD2 expression was measured by integrated density calculated in the IPL and the GCL. No significant differences were observed across all groups in the expression of SOD2 in the GCL. However, there was a trend toward increased SOD2 expression in the CPP-P1-treated group ($p=0.16$) (Supplementary Figure S1).

3.8. Assessment of RGC Survival via RBPMS-Positive Cell Analysis

To comprehensively evaluate the neuroprotective effects of CPP-P1 following SO removal, we analyzed RGC survival using RBPMS-positive cell analysis. We monitored PERG responses, integrating both structural and functional assessments to understand the retinal preservation under SO-induced stress. In this round of experiments, SO was removed from the eyes, and PERG was monitored for 3 weeks before tissue collection. Following SO injection and subsequent removal, a significant decrease in PERG amplitude was observed ($p<0.0001$). This reduction was consistent

 doi:10.20944/preprints202410.0888.v1

across rats treated with either vehicle or CPP-P1, showing minimal difference between the two groups (Figure 6A). However, analysis of PERG latency revealed that retinas treated with CPP-P1 exhibited significant preservation compared to those treated with the vehicle (Figure 6B). Images were taken from each of the 4 quadrants of the retina, and the OD (right) eyes were used as a contralateral control. The average number of RBPMS-positive cells was 1445 ± 45, 831 ± 209, and 1366 ± 154 per mm^2 for the OD eyes, the SO + vehicle OS (left) eyes, and the SO + CPP-P1 OS eyes, respectively (Figure 6C). As a result, the SO-induced IOP elevation showed approximately a 42% loss in RGCs (p=0.009), while the addition of CPP-P1 reduced this loss by about 37% (p=0.03).

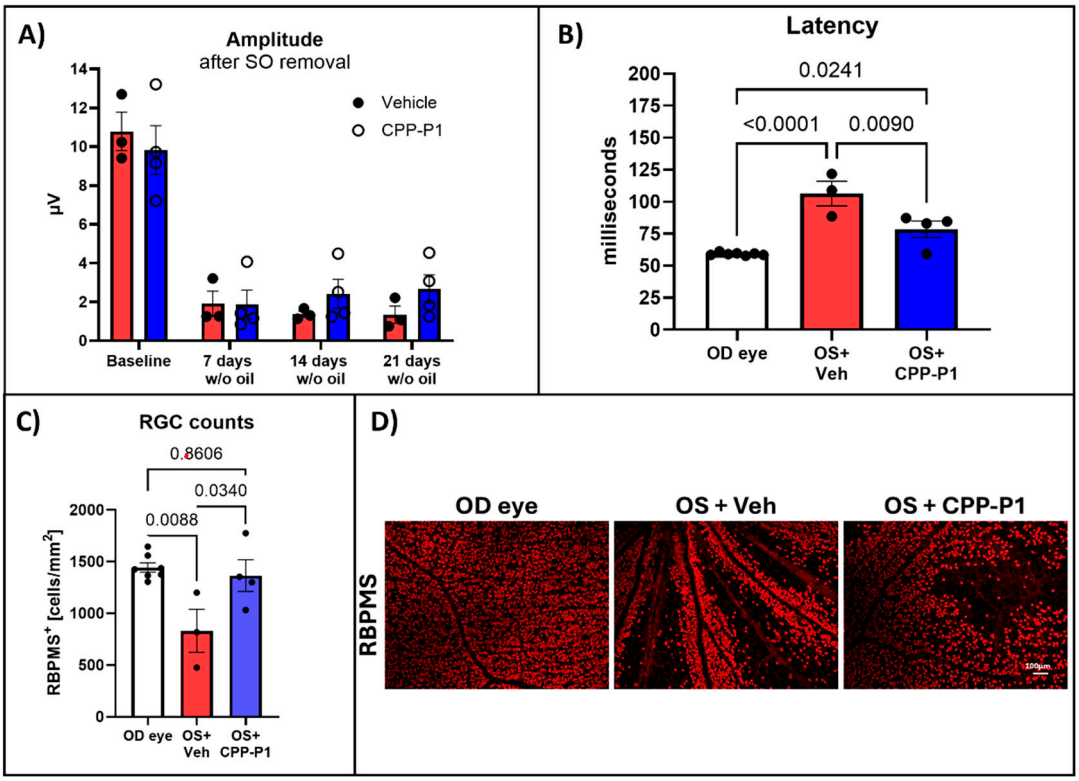

Figure 6. PERG Measurements and RBPMS-positive RGC counts following SO removal. (**a**) PERG amplitude measurements in OS eyes were recorded before SO injection (baseline) and weekly for 3 weeks after SO removal (w/o oil). (**b**) PERG latency averaged across all post-removal measurements showed a significant reduction in the response time delay of RGCs to a patterned visual stimulus. (**c**) RGC counts were obtained from RBPMS-stained retinal flat-mounts. (d) Representative images of RBPMS-stained retinas. N = 3-4 animals; statistical analysis was performed using One-way ANOVA. Images were captured at 10× magnification. The scale bar represents 100 μm.

4. Discussion

The SO model of ocular hypertension effectively induced retinal damage, as evidenced by the significant loss of RGCs and marked thinning of the ONL, INL, IPL, and GCL layers. Rats that received an intravitreal injection of CPP-P1 displayed promising indications of neuroprotection, consistent with previous studies showing its ability to preserve RGCs in other glaucoma models [22,26]. Examination of the retinal flat-mounts labeled with RBPMS revealed that the pattern of RGC degeneration induced by SO was unevenly distributed across the retina. Interestingly, RGCs located near major blood vessels appeared to survive, suggesting a potential protective effect in these regions. This distinct pattern of degeneration may be consistent with acute retinal arterial ischemia [52], possibly due to the high extent of IOP elevation used in this model.

After confirming the overall effectiveness of the SO model and the neuroprotective effects of CPP-P1, we shifted our focus to analyzing the potential mechanisms of action of CPP-P1 by evaluating the relative expression of key proteins involved in neuroprotection. CREB-mediated

 doi:10.20944/preprints202410.0888.v1

activation of neuroplasticity and neuroprotection have implications for the development of neuroprotective strategies for numerous neurodegenerative disorders, including Alzheimer's disease, Huntington's disease, amyotrophic lateral sclerosis, and Parkinson's disease [53]. Our previous study suggested that CREB signaling is activated following CPP-P1 administration [30]; therefore, the first two targets analyzed in this study were CREB and its phosphorylated form, p-CREB (Ser133). While CREB is known to promote cell survival and respond to growth factors, some markers of synaptogenesis were also implicated in CPP-P1's possible mode of neuroprotection [54–56]. Therefore, two additional markers were selected: GAP43 and SYN1. Additionally, we chose another target from a previous transcriptomic study [30], SOD2, which may further support CPP-P1's role in promoting mitochondrial health. Fluorescent microscopy was utilized using consistent settings for laser intensity, exposure time, and gain across all samples to accurately assess the relative expression of these targets. When evaluating the expression of CREB and p-CREB, the naïve group showed a low constitutive expression of CREB and a much higher (approximately 2-fold) expression of p-CREB. The ratios of activated p-CREB to CREB were consistent between the SO groups treated with CPP-P1 or vehicle. However, when examining the individual expression levels, the CPP-P1-treated group showed higher overall expressions of both CREB and p-CREB. This suggests that while CPP-P1 treatment did not appear to alter the activation ratio of p-CREB to CREB significantly, it did lead to an overall increase in the expression of both CREB and p-CREB in this acute hypertension model. Synaptogenesis markers GAP43 and SYN1 were assessed in the GCL and IPL. SYN1 binds synaptic vesicles and was primarily expressed in the IPL (where the axons of bipolar cells synapse with the dendrites of the RGCs) and the NFL – the RGC axons. A thinning of these layers was found based on the data of H&E staining and significant decreases in SYN1 expression in the SO and vehicle-treated group compared to the naïve group. GAP43 expression was similarly low in both the naïve and SO + vehicle-treated groups, and there was an increasing trend in IPL and GCL in the SO + CPP-P1-treated groups. This observation suggested a modest increase in synaptogenesis or the upregulation of proteins that support axonal health and maintenance. These proteins may promote synaptic connectivity, stabilize neural networks, or enhance axons' structural integrity, contributing to neuronal survival and function.

SOD2 is a key enzyme that provides protection against oxidative damage mediated by superoxides generated as a byproduct of mitochondrial bioenergetics and oxidative phosphorylation. The data presented here indicated that CPP-P1 had little to no effect on the SOD2 expression in the SO model. In contrast, transcriptomic data obtained in a chronic ocular hypertension model [30] suggested that more SOD2 was produced in the IOP-elevated group treated with CPP-P1 compared to the untreated IOP-elevated group. The data shown here suggests there was no increase in the protein expression level, and thus, there was no direct association between CPP-P1 treatment and SOD2 levels in the SO model. Investigating the expression at later time points, 2 to 3 weeks of IOP-elevation with weekly drug treatment, may show higher SOD2 levels upon CPP-P1 treatment. Some studies suggest that SOD2 is upregulated early in the disease processes as a compensatory mechanism, gradually decreasing over time [57,58]. Therefore, it is possible that CPP-P1 may help to sustain the elevated SOD2 expression during this period.

It is also important to acknowledge the limitations of this study. The IOP measurements were done consistently, but there has been evidence of anesthesia (e.g., isoflurane) influencing IOP [59,60]. The consistency of injury in the SO model of ocular hypertension has not yet been well characterized, and the possible variability makes the assessment of CPP-P1's efficacy difficult. Regarding the inability to accurately assess PERG when SO was present in the anterior chamber of experimental animals, the group that developed this model in mice had similar issues, noting that the "lack of progression of PERG amplitude reduction suggests SO itself may affect the light stimulation and PERG signal" [48]. Another potential limitation to consider is the form of CPP-P1 used, and a more stable mode of delivery that allows for sustained long-term release would be desirable.

 doi:10.20944/preprints202410.0888.v1

5. Conclusions

In this study, an acute SO model of glaucoma was used to provide additional evidence of the multifaceted neuroprotective nature of CPP-P1 and to investigate the cellular and signaling mechanisms of action of peptain-1. The immunohistochemical staining demonstrated an increase in overall CREB expression as well as p-CREB expression in rats treated with CPP-P1, indicating the involvement of this critical signaling pathway in CPP-P1's neuroprotective effects that include the preservation of cell counts and retinal thickness. There were trends of increased synaptogenesis (indicated by GAP43 and SYN1) and mitochondrial antioxidant response as indicated by SOD2. The retinal injury in this model was too harsh to precisely assess cell survival and preservation of function. This study provides additional evidence supporting CPP-P1's potential to be developed into a neuroprotective agent for the treatment of glaucomatous optic neuropathy as well as more acute neurodegenerative diseases, such as acute angle-closure glaucoma or central retinal artery occlusion.

Supplementary Materials: The following supporting information can be downloaded at the website of this paper posted on Preprints.org, Figure S1: Mitochondrial SOD2.

Author Contributions: Conceptualization, D.L.S., and R.H.N.; data curation, G.A.J.; formal analysis, D.L.S., and G.A.J.; funding acquisition, G.A.J., R.R.K., and R.H.N.; investigation, G.A.J.; methodology, G.A.J., and D.L.S.; project administration, D.L.S.; resources, R.R.K., and D.L.S.; supervision, D.L.S.; validation, G.A.J., and D.L.S.; visualization, G.A.J.; writing—original draft preparation, G.A.J.; writing—review and editing, G.A.J., R.R.K., R.H.N., and D.L.S.; All authors have read and agreed to the published version of the manuscript.

Funding: Funding for this research was provided by the Gates Grubstake Award (R.H.N.), Research to Prevent Blindness, NY, to the Department of Ophthalmology, University of Colorado. Funding was also provided by the Neurobiology of Aging and Alzheimer's Disease training grant: T32 AG020494 (G.A.J.). The work was supported in part by an extramural grant to R.R.K. from the National Eye Institute [R01EY028179].

Institutional Review Board Statement: The animal study protocol was approved by the Institutional Review Board of the University of North Texas Health Science Center (protocol code 2023-0024, July 2023).

Data Availability Statement: The raw data supporting the conclusions of this article will be made available by the authors on request.

Acknowledgments: We want to acknowledge lab members who contributed ideas and feedback in meetings, Calvin D. Brooks, Bindu Kodati, Ph.D., Max R. Petty, and Wei "Julie" Zhang, M.D. In addition, we extend a special thank you to Jennifer H. Pham, Ph.D., for her thorough review of the manuscript and her thoughtful input and feedback throughout the project.

Conflicts of Interest: CPP-P1 technology to treat eye diseases has been licensed to Eyegenex, Inc. from the University of Colorado, Aurora, CO 80045. RHN is the Chief Scientific Advisor to Eyegenex, Inc. The authors declare no other conflicts of interest.

References

1. Allison, K., Patel, D., & Alabi, O., Epidemiology of Glaucoma: The Past, Present, and Predictions for the Future. Cureus, 2020. 12.
2. De Moraes, C.G., J.M. Liebmann, and L.A. Levin, Detection and measurement of clinically meaningful visual field progression in clinical trials for glaucoma. Prog Retin Eye Res, 2017. 56: p. 107-147.
3. Erb, C., et al., Electrical neurostimulation in glaucoma with progressive vision loss. Bioelectron Med, 2022. 8(1): p. 6.
4. Quigley, H.A., Clinical trials for glaucoma neuroprotection are not impossible. Curr Opin Ophthalmol, 2012. 23(2): p. 144-54.
5. Akerfelt, M., R.I. Morimoto, and L. Sistonen, Heat shock factors: integrators of cell stress, development and lifespan. Nat Rev Mol Cell Biol, 2010. 11(8): p. 545-55.
6. Andley, U.P., The lens epithelium: focus on the expression and function of the alpha-crystallin chaperones. Int J Biochem Cell Biol, 2008. 40(3): p. 317-23.
7. Fischer, D., et al., Crystallins of the beta/gamma-superfamily mimic the effects of lens injury and promote axon regeneration. Mol Cell Neurosci, 2008. 37(3): p. 471-9.
8. Fort, P.E. and K.J. Lampi, New focus on alpha-crystallins in retinal neurodegenerative diseases. Exp Eye Res, 2011. 92(2): p. 98-103.

9. Piri, N., J.M. Kwong, and J. Caprioli, Crystallins in retinal ganglion cell survival and regeneration. Mol Neurobiol, 2013. 48(3): p. 819-28.
10. Rajeswaren, V., et al., Small Heat Shock Proteins in Retinal Diseases. Front Mol Biosci, 2022. 9: p. 860375.
11. Sreekumar, P.G., et al., Antiapoptotic properties of α-crystallin-derived peptide chaperones and characterization of their uptake transporters in human RPE cells. Invest Ophthalmol Vis Sci, 2013. 54(4): p. 2787-98.
12. Vendredy, L., E. Adriaenssens, and V. Timmerman, Small heat shock proteins in neurodegenerative diseases. Cell Stress & Chaperones, 2020. 25(4): p. 679-699.
13. Anders, F., et al., The Small Heat Shock Protein α-Crystallin B Shows Neuroprotective Properties in a Glaucoma Animal Model. Int J Mol Sci, 2017. 18(11).
14. Kannan, R., P.G. Sreekumar, and D.R. Hinton, Novel roles for α-crystallins in retinal function and disease. Prog Retin Eye Res, 2012. 31(6): p. 576-604.
15. Kannan, R., et al., Alpha Crystallin Derived Peptide Chaperone Protects Human RPE Cells From Oxidative Injury. Investigative Ophthalmology & Visual Science, 2010. 51(13): p. 1441-1441.
16. Kourtis, N., V. Nikoletopoulou, and N. Tavernarakis, Small heat-shock proteins protect from heat-stroke-associated neurodegeneration. Nature, 2012. 490(7419): p. 213-218.
17. Liu, H., et al., Crystallins Play a Crucial Role in Glaucoma and Promote Neuronal Cell Survival in an In Vitro Model Through Modulating Muller Cell Secretion. Invest Ophthalmol Vis Sci, 2022. 63(8): p. 3.
18. Liu, J.P., et al., Human alphaA- and alphaB-crystallins prevent UVA-induced apoptosis through regulation of PKCalpha, RAF/MEK/ERK and AKT signaling pathways. Exp Eye Res, 2004. 79(6): p. 393-403.
19. McGreal, R.S., et al., αB-crystallin/sHSP protects cytochrome c and mitochondrial function against oxidative stress in lens and retinal cells. Biochim Biophys Acta, 2012. 1820(7): p. 921-30.
20. Munemasa, Y., et al., The role of alphaA- and alphaB-crystallins in the survival of retinal ganglion cells after optic nerve axotomy. Invest Ophthalmol Vis Sci, 2009. 50(8): p. 3869-75.
21. Nahomi, R.B., et al., Chaperone peptides of α-crystallin inhibit epithelial cell apoptosis, protein insolubilization, and opacification in experimental cataracts. J Biol Chem, 2013. 288(18): p. 13022-35.
22. Nam, M.-H., et al., Peptains block retinal ganglion cell death in animal models of ocular hypertension: implications for neuroprotection in glaucoma. Cell Death & Disease, 2022. 13(11): p. 958.
23. Reddy, V.S. and G.B. Reddy, Emerging therapeutic roles of small heat shock protein-derived mini-chaperones and their delivery strategies. Biochimie, 2022.
24. Sreekumar, P.G., et al., Intra-vitreal αB crystallin fused to elastin-like polypeptide provides neuroprotection in a mouse model of age-related macular degeneration. J Control Release, 2018. 283: p. 94-104.
25. Sreekumar, P.G., et al., Mechanisms of RPE senescence and potential role of αB crystallin peptide as a senolytic agent in experimental AMD. Exp Eye Res, 2022. 215: p. 108918.
26. Stankowska, D.L., Nam, M. H., Nahomi, R. B., Chaphalkar, R. M., Nandi, S. K., Fudala, R., Krishnamoorthy, R. R., & Nagaraj, R. H., Systemically administered peptain-1 inhibits retinal ganglion cell death in animal models: Implications for neuroprotection in glaucoma. Cell Death Discovery, 2019. 5.
27. Webster, J.M., et al., Small Heat Shock Proteins, Big Impact on Protein Aggregation in Neurodegenerative Disease. Front Pharmacol, 2019. 10: p. 1047.
28. Wu, N., et al., α-Crystallin protects RGC survival and inhibits microglial activation after optic nerve crush. Life Sciences, 2014. 94(1): p. 17-23.
29. Yan, H., et al., The Protective Effects of αB-Crystallin on Ischemia-Reperfusion Injury in the Rat Retina. J Ophthalmol, 2017. 2017: p. 7205408.
30. Johnson, G.A., et al., Mechanisms contributing to inhibition of retinal ganglion cell death by cell permeable peptain-1 under glaucomatous stress. Cell Death Discovery, 2024. 10(1): p. 305.
31. Arthur, J.S., et al., Mitogen- and stress-activated protein kinase 1 mediates cAMP response element-binding protein phosphorylation and activation by neurotrophins. J Neurosci, 2004. 24(18): p. 4324-32.
32. Caracciolo, L., et al., CREB controls cortical circuit plasticity and functional recovery after stroke. Nat Commun, 2018. 9(1): p. 2250.
33. Kandel, E.R., The molecular biology of memory: cAMP, PKA, CRE, CREB-1, CREB-2, and CPEB. Mol Brain, 2012. 5: p. 14.
34. Walton, M.R. and I. Dragunow, Is CREB a key to neuronal survival? Trends Neurosci, 2000. 23(2): p. 48-53.
35. Wang, L., et al., The transcription factor CREB acts as an important regulator mediating oxidative stress-induced apoptosis by suppressing αB-crystallin expression. Aging (Albany NY), 2020. 12(13): p. 13594-13617.
36. Guo, X.J., et al., Dysregulation of neurotrophic and inflammatory systems accompanied by decreased CREB signaling in ischemic rat retina. Exp Eye Res, 2014. 125: p. 156-63.
37. Guo, X., et al., Preservation of vision after CaMKII-mediated protection of retinal ganglion cells. Cell, 2021. 184(16): p. 4299-4314.e12.

38. Zhu, S., et al., Schwann cell-derived extracellular vesicles as a potential therapy for retinal ganglion cell degeneration. J Control Release, 2023. 363: p. 641-656.
39. Eastwood, S.L. and P.J. Harrison, Synaptic pathology in the anterior cingulate cortex in schizophrenia and mood disorders. A review and a Western blot study of synaptophysin, GAP-43 and the complexins. Brain Res Bull, 2001. 55(5): p. 569-78.
40. Jin, Y., Synaptogenesis. WormBook, 2005: p. 1-11.
41. Kaneda, M., et al., Growth-associated protein43 (GAP43) is a biochemical marker for the whole period of fish optic nerve regeneration. Adv Exp Med Biol, 2010. 664: p. 97-104.
42. Cho, K.S., et al., Re-establishing the regenerative potential of central nervous system axons in postnatal mice. J Cell Sci, 2005. 118(Pt 5): p. 863-72.
43. Leon, S., et al., Lens injury stimulates axon regeneration in the mature rat optic nerve. J Neurosci, 2000. 20(12): p. 4615-26.
44. John, A., et al., The neurodevelopmental spectrum of synaptic vesicle cycling disorders. J Neurochem, 2021. 157(2): p. 208-228.
45. Parenti, I., et al., The different clinical facets of SYN1-related neurodevelopmental disorders. Front Cell Dev Biol, 2022. 10: p. 1019715.
46. Ferreira, S.M., et al., Oxidative stress markers in aqueous humor of glaucoma patients. American Journal of Ophthalmology, 2004. 137(1): p. 62-69.
47. Ghanem, A.A., L.F. Arafa, and A. El-Baz, Oxidative Stress Markers in Patients with Primary Open-Angle Glaucoma. Current Eye Research, 2010. 35(4): p. 295-301.
48. Zhang, J., et al., Silicone oil-induced ocular hypertension and glaucomatous neurodegeneration in mouse. Elife, 2019. 8.
49. Fang, F., et al., Chronic mild and acute severe glaucomatous neurodegeneration derived from silicone oil-induced ocular hypertension. Scientific Reports, 2021. 11(1): p. 9052.
50. Zhang, J., et al., A Reversible Silicon Oil-Induced Ocular Hypertension Model in Mice. J Vis Exp, 2019(153).
51. Kodati, B., et al., Oral administration of a dual ET(A)/ET(B) receptor antagonist promotes neuroprotection in a rodent model of glaucoma. Mol Vis, 2022. 28: p. 165-177.
52. Dattilo, M., N.J. Newman, and V. Biousse, Acute retinal arterial ischemia. Annals of Eye Science, 2018. 3: p. 28.
53. Khakha, N., et al., Therapeutic implications of phosphorylation- and dephosphorylation-dependent factors of cAMP-response element-binding protein (CREB) in neurodegeneration. Pharmacol Rep, 2023. 75(5): p. 1152-1165.
54. Fontanella, R.A., et al., Tirzepatide prevents neurodegeneration through multiple molecular pathways. J Transl Med, 2024. 22(1): p. 114.
55. Jiang, Y.Y., et al., Ginsenoside Rg1 promotes neurite growth of retinal ganglion cells through cAMP/PKA/CREB pathways. J Ginseng Res, 2024. 48(2): p. 163-170.
56. Yan, D., et al., Subchronic Acrylamide Exposure Activates PERK-eIF2α Signaling Pathway and Induces Synaptic Impairment in Rat Hippocampus. ACS Chem Neurosci, 2022. 13(9): p. 1370-1381.
57. Naguib, S., et al., Retinal oxidative stress activates the NRF2/ARE pathway: An early endogenous protective response to ocular hypertension. Redox Biol, 2021. 42: p. 101883.
58. Jiang, W., et al., Adeno-associated virus mediated SOD gene therapy protects the retinal ganglion cells from chronic intraocular pressure elevation induced injury via attenuating oxidative stress and improving mitochondrial dysfunction in a rat model. Am J Transl Res, 2016. 8(2): p. 799-810.
59. Chae, J.J., M.R. Prausnitz, and C.R. Ethier, Effects of General Anesthesia on Intraocular Pressure in Rabbits. J Am Assoc Lab Anim Sci, 2021. 60(1): p. 91-95.
60. Tsuchiya, S., et al., Effect of inhalation anesthesia with isoflurane on circadian rhythm of murine intraocular pressure. Exp Eye Res, 2021. 203: p. 108420.